PROCEEDINGS OF SCIENCE

# Search for SM Higgs decaying to $WW \to \ell\nu\ell\nu$ and $\ell\nu\, qq$ at CMS

**Emanuele Di Marco***
On behalf of the CMS Collaboration
*California Institute of Technology*
*E-mail:* emanuele.di.marco@cern.ch

A search for the standard model Higgs boson decaying to $W^+W^-$. The pp collisions data sample corresponds to an integrated luminosity of 5.1 fb$^{-1}$ at $\sqrt{s}$ = 7 TeV and 5.1 fb$^{-1}$ at $\sqrt{s}$ = 8 TeV, collected by the CMS detector at the LHC. The $W^+W^-$ candidates are selected in events in the fully leptonic or semi leptonic final state. Upper limits on the Higgs boson production relative to the standard model Higgs expectation are derived. The standard model Higgs boson is excluded in the mass range 129–520 GeV at 95% confidence level from the fully leptonic channel and in the mass ranges 260–460 GeV from the semi-leptonic channel. A 1.6 $\sigma$ (2.4 $\sigma$) excess of events is observed (expected) for low Higgs boson masses which makes the observed limits weaker than the expected ones under the null hypothesis.

*36th International Conference on High Energy Physics,*
*July 4-11, 2012*
*Melbourne, Australia*

*Speaker.

 

## 1. Introduction

One of the open questions in the standard model (SM) of particle physics is the origin of the masses of fundamental particles. Within the SM, vector boson masses arise from the spontaneous breaking of electroweak symmetry by the Higgs field [1, 2]. The existence of the associated field quantum, the Higgs boson, has yet to be established experimentally. The discovery or the exclusion of the SM Higgs boson is one of the central goals of the CERN Large Hadron Collider (LHC) physics program. In this conference I reported about the search for the Higgs boson in the $H \to W^+W^- \to 2\ell 2\nu$ and $H \to W^+W^- \to \ell\nu 2q$ final states, where $\ell$ is a charged lepton, electron or muon, $\nu$ a neutrino, and $q$ a quark. The first analysis is performed in the mass range 110–600 GeV, while the second, which needs a high $p_T$ lepton to trigger the W decaying leptonically, is only performed in the mass range 170–600 GeV. The search discussed here is performed using the data sample corresponding to $5.1 \pm 0.2$ fb $^{-1}$ of integrated luminosity collected in 2012 at a center-of-mass energy of 8 TeV. Finally, the $\sqrt{s} = 7$ TeV data sample is added to the analysis to obtain the combined 2011 and 2012 results. The data collected by CMS detector, a multipurpose apparatus designed to study high transverse momentum ($p_T$) physics processes in proton-proton collisions (described in detail in [3]), are used.

## 2. Physics objects for $W^+W^- \to \ell\nu\ell\nu$ and $W^+W^- \to \ell\nu qq$ event selection

The search strategy for $H \to W^+W^- \to \ell\nu\ell\nu$ is based on a signature with two isolated, oppositely charged, high $p_T$ leptons (electrons or muons) and large missing transverse momentum, $E_T^{miss}$, due to the undetected neutrinos. To improve the signal sensitivity, the events are separated by jet multiplicity into three mutually exclusive categories. The search strategy for $H \to W^+W^- \to \ell\nu 2q$ is based on the final state with one high $p_T$ lepton (electron or muon), large $E_T^{miss}$ and two or three jets due to the hadronic decay of the W and one possible additional jet in the event. In the $W^+W^- \to \ell\nu\ell\nu$ analysis the events are selected by triggers which require the presence of one or two high-$p_T$ electrons or muons. For the semi-leptonic channel, a suite of single lepton triggers mostly using transverse momentum thresholds of 24 GeV for muons and 27 GeV for electrons is used.

Muon candidates are identified using a selection similar to the one described in [4]. Muons are required to be isolated to distinguish between muon candidates from W-boson decays and those from QCD background processes, which are usually in or near jets. For each muon candidate, the scalar sum of the transverse energy of all particles compatible with originating from the primary vertex is reconstructed in cones of several widths around the muon direction. Electron candidates are identified using a multivariate approach based on variables similar to those described in [5] and exploiting information from the tracker, the ECAL, and the combination of these two detectors. Electrons are required to be isolated by applying a threshold on the sum of the transverse energy of the particles which are reconstructed in a cone around them. For both electrons and muons a correction is applied to account for the contribution to the energy in the isolation cone from the pile-up using the measured median energy density in the event. They are required to originate from the primary vertex of the event.

Jets are reconstructed using the anti-$k_T$ clustering algorithm [6] with distance parameter $\Delta R = 0.5$. A similar correction as for the lepton isolation is applied to account for the contribution to the jet energy from the pile-up. Jet energy corrections are applied as a function of the jet $E_T$ and $\eta$. A selection is applied to separate jets from the primary interaction from those reconstructed due to energy deposits associated with pile-up, based on the differences in the jet shapes, in the relative multiplicity of charged and neutral components and in the different fraction of transverse momentum which is carried by the hardest components. Within the tracker acceptance the jet tracks are also required to be compatible with the primary vertex. Events are classified according to the number of selected jets with $E_T > 30$ GeV and $|\eta| < 4.7$.

In addition to high momentum isolated leptons and minimal jet activity missing transverse momentum is present in signal events due to $W \to \ell\nu$ decays. For the $W^+W^- \to \ell\nu\ell\nu$ final state with same-flavor leptons, a large background comes from Drell-Yan process, where no real $E_T^{miss}$ is present. In this case a *projected* $E_T^{miss}$ variable is employed. It is equal to the component of $E_T^{miss}$ transverse to the nearest lepton if the difference in azimuth between this lepton and the $E_T^{miss}$ vector is less than $\pi/2$. If there is no lepton within $\pi/2$ of the direction of $E_T^{miss}$ in azimuth, $E_T^{miss}$ is used directly. Since the *projected* $E_T^{miss}$ resolution is degraded by pile-up, the minimum of two $E_T^{miss}$ observables is used: the first includes all reconstructed particles in the event, while the second uses only the charged particles associated with the primary vertex. In the semi-leptonic final state, since the main background arises from associated W and jets production with real $E_T^{miss}$, no projection is needed.

## 3. $H \to W^+W^- \to \ell\nu\ell\nu$ search strategy

Two oppositely charged lepton candidates are required, with $p_T > 20$ GeV for the leading lepton ($p_T^{\ell,max}$) and $p_T > 10$ GeV for the trailing lepton ($p_T^{\ell,min}$). Only electrons (muons) with $|\eta| < 2.5$ (2.4) are considered in the analysis. Events with *projected* $E_T^{miss}$ above 20 GeV are selected for the analysis. To suppress the top-quark background, a *top tagging* technique based on soft-muon and b-jet tagging [7] is applied. The first method is designed to veto events containing muons from b-quarks coming from top-quark decays. The second method uses b-jet tagging algorithm which looks for tracks with large impact parameter within jets. A minimum dilepton transverse momentum ($p_T^{\ell\ell}$) of 45 GeV is required to reduce the W + jets background. To reduce the background from WZ production, any event that has a third lepton passing the identification and isolation requirements is rejected. The contribution from $W\gamma$ production, where the photon is misidentified as an electron, is reduced by about 90% in the dielectron final state by $\gamma$ conversion rejection requirements. The contribution from $W\gamma^*$ is reduced by the veto on the presence of a third lepton and by isolation requirements. The background from low mass resonances is rejected by requiring a dilepton mass ($m_{\ell\ell}$) greater than 12 GeV. The Drell-Yan process produces same-flavor lepton pairs ($e^+e^-$ and $\mu^+\mu^-$). In order to suppress this background, a few additional cuts are applied in the same-flavor final states. First, the resonant component of the Drell-Yan production is rejected by requiring a dilepton mass outside a 30 GeV window centered on the Z pole. Then, the remaining off-peak contribution is suppressed by exploiting different $E_T^{miss}$-based approaches depending on the number of jets and the Higgs mass hypothesis. At large Higgs masses ($m_H > 140$ GeV), signal events are associated with large $E_T^{miss}$, thus it is sufficient to require the minimum of the two

*projected* $E_{\mathrm{T}}^{\mathrm{miss}}$ variables to be greater than 45 GeV. For $m_{\mathrm{H}} \leq 140$ GeV analysis, a dedicated multivariate selection combining missing transverse momentum, kinematic and topological variables, is used. In events with two jets the dominant source of fake $E_{\mathrm{T}}^{\mathrm{miss}}$ is the mismeasurement of the hadronic recoil, thus $E_{\mathrm{T}}^{\mathrm{miss}} > 45$ GeV is sufficient. Finally, the momenta of the dilepton system and of the most energetic jet must not be back-to-back in the transverse plane. These selections effectively reduce the Drell-Yan background by three orders of magnitude, while rejecting less than 50% of the signal.

After applying the full set of selection criteria described in this section, referred to as the $\mathrm{W^+W^-}$ selection, the observed yields in data are 1594, 1186, and 1295 events in the 0-jet, 1-jet, and 2-jet categories respectively. This sample is dominated by non-resonant $\mathrm{W^+W^-}$ events. To enhance the sensitivity to a Higgs boson signal, a cut-based approach is chosen for the final Higgs selection. Because the kinematics of signal events change as a function of the Higgs mass, separate optimizations are performed for different $m_{\mathrm{H}}$ hypotheses. The extra requirements, designed to optimize the sensitivity for a SM Higgs boson, are placed on $p_{\mathrm{T}}^{\ell,\mathrm{max}}$, $p_{\mathrm{T}}^{\ell,\mathrm{min}}$, $m_{\ell\ell}$, $\Delta\phi_{\ell\ell}$ and the transverse mass $m_{\mathrm{T}}$, defined as $\sqrt{2p_{\mathrm{T}}^{\ell\ell}E_{\mathrm{T}}^{\mathrm{miss}}(1-\cos\Delta\phi_{E_{\mathrm{T}}^{\mathrm{miss}}\ell\ell})}$, where $\Delta\phi_{E_{\mathrm{T}}^{\mathrm{miss}}\ell\ell}$ is the difference in azimuth between $E_{\mathrm{T}}^{\mathrm{miss}}$ and the transverse momentum of the dilepton system. The $\Delta\phi_{\ell\ell}$ and $m_{\ell\ell}$ distributions in the 0-jet category, for a $m_{\mathrm{H}} = 125$ GeV SM Higgs boson and for the main backgrounds are shown in Figure 1. The clear difference in the shape between the $\mathrm{H} \to \mathrm{W^+W^-}$ and the non-resonant $\mathrm{W^+W^-}$ processes is due to the spin-0 nature of the Higgs boson.

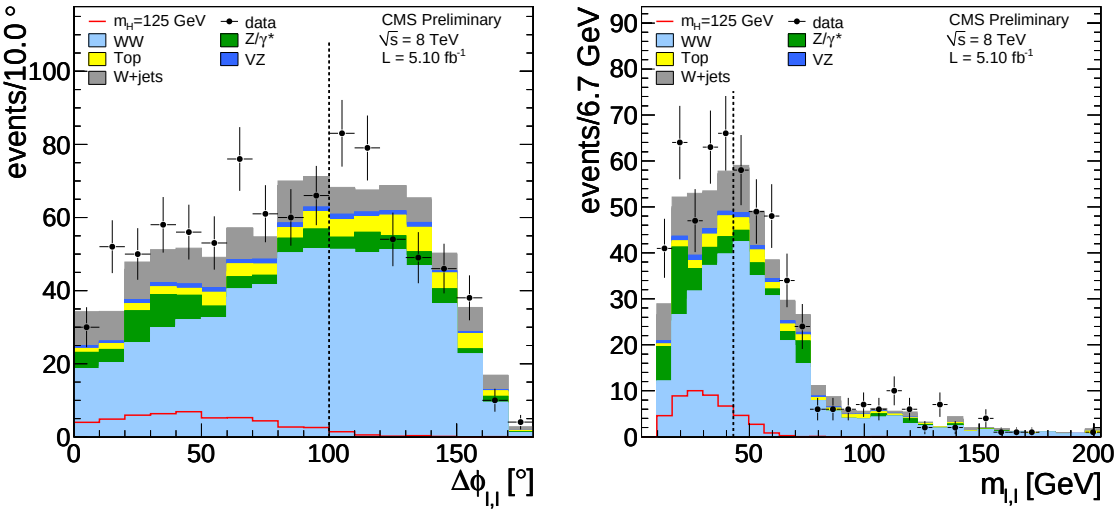


**Figure 1:** Distributions of $\Delta\phi_{\ell\ell}$ (left) and dilepton mass (right) in the 0-jet category, for a $m_{\mathrm{H}} = 125$ GeV SM Higgs boson and for the main backgrounds. The cut-based $\mathrm{H} \to \mathrm{W^+W^-}$ selection, except for the requirements on the $\Delta\phi_{\ell\ell}$ and the dilepton mass, is applied (left) and dilepton mass (right). The vertical lines indicate the cut values.

The 2-jet category is mainly sensitive to the vector boson fusion (VBF) production mode [8], whose cross section is roughly ten times smaller than that of the gluon-gluon fusion mode. The VBF signal can be extracted using extra selection criteria, providing additional search sensitivity. The $\mathrm{H} \to \mathrm{W^+W^-}$ events from VBF production are characterized by a pair of energetic forward-

backward jets and very little hadronic activity in the rest of the event. Events passing the $W^+W^-$ criteria are further required to satisfy $p_T > 30$ GeV for both leading jets, with no jets above this threshold present in the pseudorapidity region between the two leading jets. The two leptons are required to be within the pseudorapidity region defined by the two jets. To reject the main background from top-quark decays, two additional requirements are applied to the two jets, $j_1$ and $j_2$: $|\Delta\eta(j_1, j_2)| > 3.5$ and $m_{j_1 j_2} > 450$ GeV. In addition, $m_T$ is required to be larger than 30 GeV and smaller than the Higgs mass hypothesis. Finally, a $m_H$ dependent upper limit on the dilepton mass is applied.

A combination of techniques is used to determine the contributions from the background processes that remain after the Higgs selection. Where feasible, background contributions are estimated directly from data, avoiding large uncertainties related to the simulation of these sources. The remaining contributions taken from simulation are small. The W + jets and QCD multi-jet backgrounds arise from leptonic decays of heavy quarks, hadrons misidentified as leptons, and electrons from photon conversion. The estimate of these contributions is derived directly from data using a control sample of events in which one lepton passes the standard criteria and the other does not, but instead satisfies a relaxed set of requirements, resulting in a "tight-fail" sample. The efficiency, for a jet that satisfies the loose selection to pass the tight selection is determined using data from an independent multi-jet event sample dominated by non-prompt leptons and used to extrapolate the "tight-fail" counts into the signal region ("tight-tight" sample). Systematic uncertainties of this method is estimated to be about 36%. The normalization of the top-quark background is estimated from data as well by counting the number of top-tagged events and applying the corresponding top-tagging efficiency measured on data with one b-tagged jet. The main uncertainty comes from the statistical uncertainty in the control sample and from the systematic uncertainties related to the measurement of the tagging efficiency (about 20% in the 0-jet category and about 5% in the 1-jet category). For the low-mass $H \to W^+W^-$ signal region, $m_H \leq 200$ GeV, the non-resonant $W^+W^-$ contribution is estimated from data. This contribution is measured using events with a dilepton mass larger than 100 GeV, where the Higgs boson signal contamination is negligible, and a simulation is used to extrapolate into the signal region. The total uncertainty is about 10%. For larger Higgs boson masses there is a large overlap between the non-resonant $W^+W^-$ and Higgs boson signal, and simulation is used for the estimation. The $Z/\gamma^* \to \ell^+\ell^-$ contribution to the $e^+e^-$ and $\mu^+\mu^-$ final states is based on extrapolation from the observed number of events with a dilepton mass within $\pm 7.5$ GeV of the Z mass, where the residual background in that region is subtracted using $e^\pm\mu^\mp$ events. The largest uncertainty in the estimate is the statistical uncertainty of the control sample, which is about 20% to 50%. The $Z/\gamma^* \to \tau^+\tau^-$ contamination is estimated using $Z/\gamma^* \to e^+e^-$ and $\mu^+\mu^-$ events selected in data, where the leptons are replaced with simulated $\tau$ decays, thus providing a better description of the experimental conditions with respect to the simulation. Finally, to estimate the normalization of $W\gamma^*$ background contribution from asymmetric virtual photon decays, where one lepton escapes detection, a control sample of high purity $W\gamma^*$ events with three reconstructed leptons is used. A measured factor of $1.6 \pm 0.5$ with respect to the leading order cross section is found. Other minor backgrounds from WZ, ZZ (when the two selected leptons come from different bosons) and $W\gamma$ are estimated from simulation.

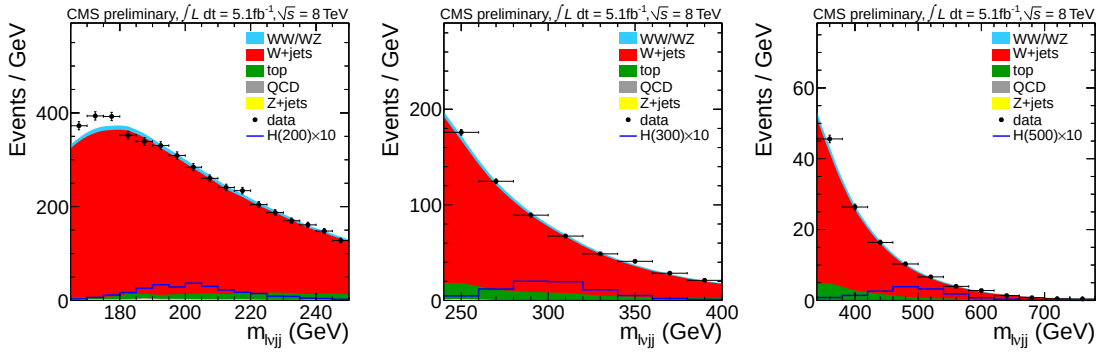


**Figure 2:** The WW invariant mass distribution with the fit projections in the signal region 65 GeV $< m_{jj} <$ 95 GeV, for the muon 2-jet category, after selections optimized for the Higgs mass hypotheses of 200 GeV (left), 300 GeV (middle), and 500 GeV (right).

## 4. $H \to W^+W^- \to \ell\nu qq$ search strategy

The combination of the two highest $p_T$ jets is chosen as the hadronic W candidate. The events with the incorrect dijet combination comprise a broad non-peaking background in the WW mass spectrum. The leptonic W candidate is reconstructed from the lepton plus $E_T^{miss}$ system. We require $E_T^{miss} > 25$ (30) GeV for each event in the muon (electron) data. The transverse mass of the leptonic W candidate is defined as $M_T \equiv \sqrt{2\, p_T^l\, E_T^{miss}\, (1-\cos(\phi_l - \phi_{E_T^{miss}}))}$, where $\phi_l$ and $\phi_{E_T^{miss}}$ are the azimuthal angles of the lepton and $E_T^{miss}$, respectively. The transverse mass $M_T$ is required to be larger than 30 GeV. The main background after this selection is due to the production of W bosons in association with jets. The requirement 65 GeV $< m_{jj} <$ 95 GeV, which keeps about 80% of the signal events, is subsequently applied in order to reduce this background. To exploit the differences in kinematics between signal and background, a likelihood discriminant is constructed that incorporates a set of five angular variables that best distinguishes the Higgs signal from the W+jets background, optimized for several Higgs mass points. The four-body mass shape of the W+jets contribution is extracted from data as a mixture of the shape measured in two signal-free regions: 95 GeV $< m_{jj} <$ 115 GeV and 55 GeV $< m_{jj} <$ 65 GeV. The four-body mass shape for multi-jet background events is obtained from data as well, by selecting a control sample of non-isolated leptons and relaxing the $E_T^{miss}$ threshold and identification requirements. For all the other backgrounds the Monte Carlo prediction is used. The $m_{\ell\nu jj}$ invariant mass distribution in the signal region is shown in Figure 2 for muon plus 2-jet final state with selections optimized for Higgs mass hypotheses of 200 GeV, 300 GeV, and 500 GeV.

## 5. Results

Upper limits are derived on the ratio of the product of the Higgs boson production cross section and the $H \to W^+W^-$ branching fraction, $\sigma_H \times BR(H \to W^+W^-)$, and the SM Higgs expectation, $\sigma/\sigma_{SM}$. To compute the upper limits the modified frequentist construction $CL_s$ [9] is used. The 95% CL observed and expected median upper limits are shown in Fig. 3. The bands represent the $1\sigma$ and $2\sigma$ probability intervals around the expected limit. The 8 TeV $W^+W^- \to \ell\nu\ell\nu$ analysis

excludes the presence of a Higgs boson with mass in the range 135–198 GeV at 95% CL, while the expected exclusion limit in the hypothesis of background only is 128–250 GeV. With the addition of the 7 TeV analysis, a Higgs boson with mass in the range 129–520 GeV is excluded at 95% CL, while the expected exclusion limit for the background only hypothesis is in the range 122–450 GeV. The observed (expected) upper limits are about 2.2 (1.2) times the SM expectation for $m_{\mathrm{H}} = 125$ GeV. A small excess of events is observed for hypothetical low Higgs boson masses, which makes the observed limits weaker than the expected ones. The expected significance for a SM Higgs of mass 125 GeV is 2.4 $\sigma$ and the observed significance is 1.6 $\sigma$. Due to the poor mass resolution of this channel the excess extends over a large mass range.

With the $\mathrm{W}^+\mathrm{W}^- \to \ell\nu qq$ analysis, the presence of a SM Higgs boson in the mass range $260 - 460$ GeV is excluded at 95% CL by analyzing 8 TeV data. Combining with 7 TeV results, a SM Higgs boson is excluded in the mass range $230 - 480$ GeV, at 95% confidence level. The results are shown in Fig. 3.

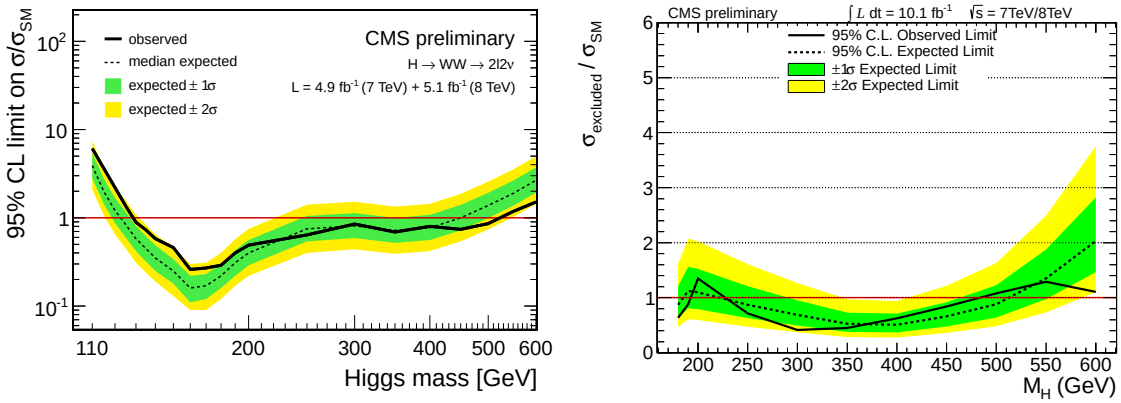


**Figure 3:** Expected and observed 95% CL upper limits on the cross section times branching fraction, $\sigma_{\mathrm{H}} \times \mathrm{BR}(\mathrm{H} \to \mathrm{W}^+\mathrm{W}^-)$, relative to the SM Higgs expectation, using the combined 7 TeV and 8 TeV data for $WW \to \ell\nu\ell\nu$ analysis (left) and $\mathrm{W}^+\mathrm{W}^- \to \ell\nu qq$ analysis (right). Results are obtained using the $\mathrm{CL}_s$ approach.

## References


[1] P. W. Higgs, Phys. Rev. Lett. **13**, 508 (1964).

[2] F. Englert and R. Brout, Phys. Rev. Lett. **13**, 321 (1964).

[3] S. Chatrchyan *et al.* [CMS Collaboration], JINST **3**, S08004 (2008).

[4] S. Chatrchyan *et al.* [CMS Collaboration], Phys. Lett. B **710**, 91 (2012)

[5] [CMS Collaboration], CMS-PAS-EGM-10-004.

[6] M. Cacciari, G. P. Salam and G. Soyez, JHEP **0804**, 063 (2008)

[7] [CMS Collaboration], CMS-PAS-BTV-09-001.

[8] M. Ciccolini, A. Denner and S. Dittmaier, Phys. Rev. Lett. **99**, 161803 (2007)

[9] A. L. Read, J. Phys. G **28**, 2693 (2002).